

*Optical Measurements*

*Paper 18*

***INVESTIGATION OF TURBULENT FLOW BY  
MEANS OF THE PIV METHOD***

*J. Schabacker, A. Bölcs*

*Laboratoire de Thermique appliquée et de Turbomachines (LTT)  
Swiss Federal Institute of Technology  
CH-1015 Lausanne*

# Investigation of turbulent flow by means of the PIV method

J.Schabacker, A. Bölcs

Laboratoire de Thermique appliquée et de Turbomachines (LTT)  
Swiss Federal Institute of Technology  
1015 Lausanne, Switzerland

## Abstract

Instantaneous flow field measurements by means of the PIV method can be employed for the reduction of mean velocities and turbulence quantities. The present paper describes the setup of a test rig and a PIV system for the study of the flow characteristics of a three dimensional flow in an internal gasturbine cooling passage.

## 1 Introduction

Non-intrusive optical techniques are widely used in fluid mechanics. During the last three decades new methods have been developed. Many of these techniques are qualitative in nature but they are of great value in guiding subsequent quantitative studies (Lauterborn 1984). An important achievement of modern experimental fluid mechanics is the invention and development of techniques for the measurement of whole, instantaneous fields of scalars and vectors. These techniques include laser-speckle velocimetry, particle-tracking velocimetry, molecular-tracking velocimetry and particle-image velocimetry (PIV) for velocity fields (Adrian 1991).

PIV in its traditional concept uses a pulsed laser light source. The light of the laser is shaped into a light sheet illuminating particles in the fluid. The particles scatter light into a photographic lens orientated at  $90^\circ$  with respect to the light sheet. The flow images are recorded either on photographic film or on the CCD of a video camera. The subsequent analysis subdivides the images into small areas. The local velocity in such an interrogation spot is determined by calculating the average particle displacement. In the Photo PIV case the images are double exposed and the task

is performed by convoluting the brightness distribution in the interrogation region with itself. For Video PIV, the particle images due to the two illuminations are stored on two consecutive video frames and the cross-correlation of the interrogation spots yields the particle displacement. The vector field is obtained by repeating the process on a grid of such interrogation spots.

An important advantage of PIV compared to other measurement techniques is its capability to obtain spatial information about the instantaneous velocity components in unsteady flows. Whereas, accepted fluid measurement practice reports time-averaged velocity and turbulence properties at a single point in space. For complex flow, the measuring time for these single point techniques can become unacceptable long. PIV measurements, on the other side can yield a large amount of whole flow field data in a rather short measuring time. A subsequent calculation of the ensemble average for identical spatial windows over many images can yield to results that allow a comparison with other results obtained from single point flow field measurement techniques. Furthermore from a combination of different measurement planes information on the quasi three-dimensional structure of the flow can be obtained.

## 2 Experimental Setup

### 2.1 Test Facility

A sketch of the test section is shown in Figure 1. The air to the test rig is supplied by a continuously running isothermal compressor driven by a 700 kW electrical motor. The mass flow rate is measured by means of an orifice meter. The air enters the settling chamber via a

150 mm tube and a conical entrance section with an angle of 30°. The inner diameter of the settling chamber is 600 mm. The settling chamber is equipped with a combination of perforated plates, honeycombs and meshes to reduce unsteadiness and swirl in the flow. For the PIV experiments 1-3  $\mu\text{m}$  oil droplets generated by a Polytec L2F-A-1000 Aerosol Generator are injected upstream of the settling chamber. This guarantees an homogeneous seeding density in the test section.

Presently the test rig is equipped with the model of a two-pass cooling passage of a gas turbine blade. The passage has a 100x100 mm cross section and a length of 2000 mm. The use of glass as a design material for the entire test section implies some difficulties since the tolerances for the fabrication of glass parts are rather large ( $\pm 1\text{mm}$ ). However, these difficulties have to be weighed against the better optical properties of glass for the performance of PIV experiments in comparison to perspex or plexiglass.

The flow path of the fluid in the test section is depicted in Figure 1. The air enters the section through a bell mounted entrance section. The sharp 180° turn is located 18 hydraulic diameters downstream of the entrance. The total section including the bell mounted section entrance can be turned 90° without changing the flow conditions in the duct. This allows an easy optical access to the positions of interest for the PIV measurements.

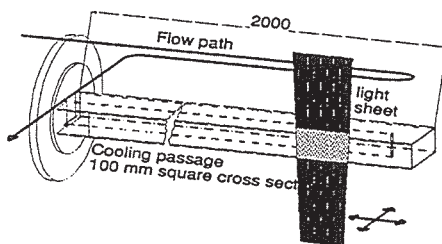


**Figure 1** The internal cooling test facility

## 2.2 PIV System

For the investigation of flow fields by means of the PIV technique several

systems have been described in the literature (Grant 1994).

One basically distinguishes between Video PIV systems and Photo PIV systems. In the Photo PIV case the images are stored on photographic film. The data reduction is performed either by means of a negative interrogation system or nowadays by a digitization of the images with a slide scanner. Video PIV systems employ CCD video cameras for the recording of the flow.

Figure 2 shows the optical arrangement of the PIV system at LTT. The laser used for the experiments is a Quantel TwinsB Nd-Yag high energy pulsed laser. The time delay between the pulses can be adjusted from 1  $\mu\text{s}$  to 1 s. The laser provides light pulses with a maximum energy of 320 mJ at a wavelength of 532 nm. The pulse duration is approximately 5 ns giving a peak power of 64 MW. A plano-concave lens (-30 mm focal length) combined with two plano-cylindrical lenses (76.2 and 300 mm focal length) transform the beam into a thin vertical light sheet. The thickness and width of the light sheet can both be adjusted by an appropriate distance between lenses. All lenses have an anti-reflection coating.

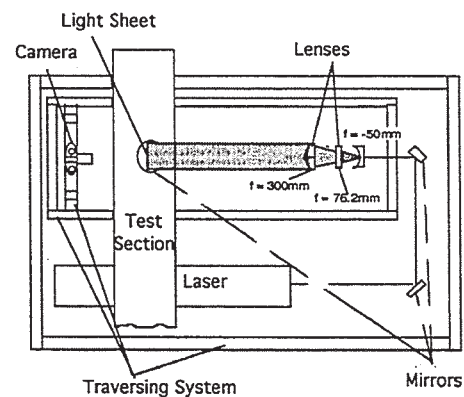


**Figure 2** The PIV setup

A 35 mm camera with a 60 mm macro planar Zeiss lens records double exposed images on a KODAK Tmax 3200 film. The camera was designed by DLR Göttingen (Germany). It consists of a Yashica camera body with a CCD sensor mounted in the viewfinder. The position of the CCD sensor is carefully aligned so that the distance between lens and the sensor, via the mirror, is exactly

the same as that between the lens and the film plane. The CCD allows one to view a small area of the flow, with the spatial resolution being approximately the same as the resolution of the film. The video signal from the CCD sensor is transmitted to a PC via a Data Translation DT3852 frame grabber board. The particle images show up on the screen and both the camera position as well as the particle displacement can be controlled.

The complete system including laser, light sheet optics and camera is mounted on a traversing system that allows a easy displacement to the position of interest.

For the analysis, the PIV images are scanned by means of a Nikon Coolscan LS-1000 film scanner. The scanner is equipped with an auto slide feeder that allows the digitization of a series of 50 slides per hour. The scanner has a resolution of 2700 dpi. This corresponds to a pixel density of 106 pixels/mm on the film. For a typical PIV recording the imagefile size is about 7 MB. These images are saved as TIFF files on the PC.

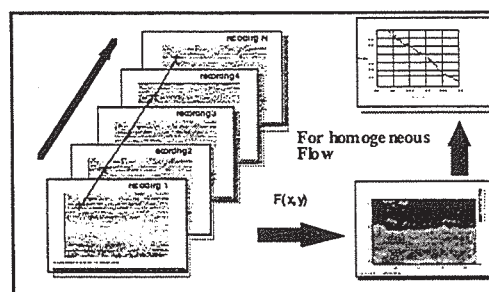
For a statistical investigation of PIV measurements one has to be sure that a single point in space on the film matches the same point in the flow for the entire series of PIV recordings. During previous tests with the system, uncertainties in locating the position of a marker in the flow of about 2.5% of the image height were observed. These displacements of the images are due to the transport of the film inside the camera as well as because of the subsequent framing of the slides and the digitalisation with the film scanner. For this reason the images are aligned after the digitization according to the position of a marker in the flow field.

The images are interrogated with the PIV software package VISIFLOW, from AEA Technology. An autocorrelation method is used with an interrogation spot size of 128 by 128 pixels and 50 % overlap. A single interrogation is performed in less than 0.5 sec on a 150 MHz Pentium PC. The analysis of a typical PIV recording (1500 vectors) takes less than 12 minutes. Usually the

data contain a small number ( less than 1 % ) of spurious vectors. The vector field is then validated with pre-defined thresholds. The invalid velocity vectors are replaced and the remaining gaps are filled by a weighted average of surrounding vectors.

### 3. Statistical Investigation of PIV Recordings

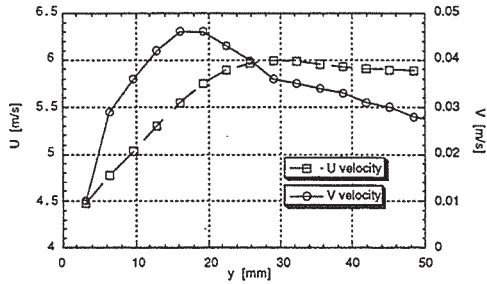
Engineers are interested not only in instantaneous flow phenomena but also in mean velocity field and turbulence quantities of a flow. Since PIV measurements can help decrease testing time the calculation of these flow properties from the originally instantaneous measurements is worthwhile. Therefore, an ensemble average of the velocity data in identical spatial windows in a series of PIV recordings is calculated (Figure 3). For homogeneous flow those ensemble averages again can be averaged along lines parallel to the main stream direction. Each image can be thought of as an independent sample of the velocity field and statistical sampling theory can be used to predict the confidence interval with which the data is reported.



**Figure 3** Statistical investigation of series of PIV recordings

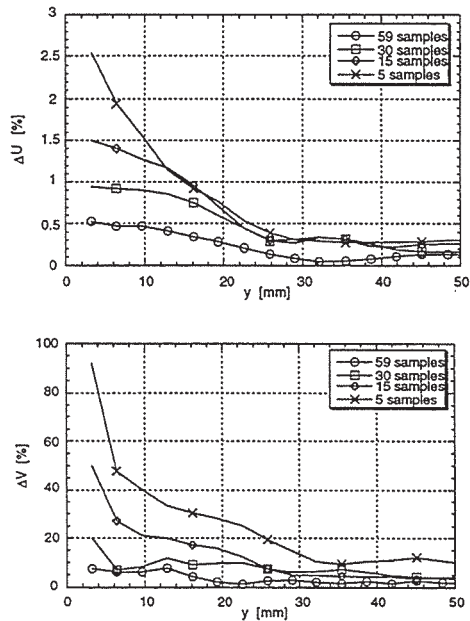
The number of PIV recordings necessary to obtain flow parameters for a given accuracy is one principle consideration in sampling theory.

Figure 4 shows profiles of the stream-wise and transverse mean velocities in the center-plane 16 hydraulic diameters downstream from the duct entrance.



**Figure 4** Streamwise and transverse mean velocity profiles

The flow parameters were calculated from a sample of 120 PIV recordings. Then four groups of 59 recordings sample size, four groups of 30 recordings, 8 groups of 15 recordings and 24 groups of 5 recordings were created from the total sample. In Figure 5 the profiles of the fractional error in function of the sample size for the streamwise and transverse mean velocity are shown.



**Figure 5** Fractional error in the estimation of streamwise and transverse mean velocity

For the horizontal velocity rather small samples sizes are sufficient. A sample size of five recordings yields predictions within a maximal deviation of 2.5%. The measurements of the transverse velocity are affected by a higher inaccuracy due to the smaller magnitude. The fractional error is higher and

therefore a larger sample size is necessary for results to be reported with the same uncertainty as that obtained for the transverse velocity component.

Figure 6 shows the turbulence intensity profile and the associated fractional error. The fractional error in estimating the turbulence intensity is rather high in comparison to the prediction of the mean velocities. This indicates that for reliable measurements of turbulence quantities far more than 120 PIV images are required

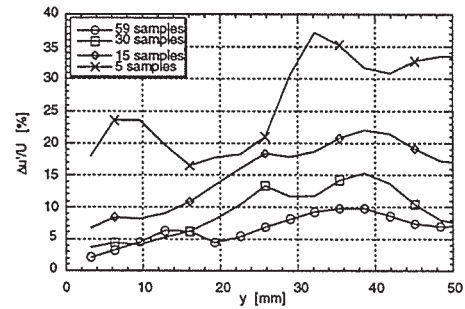
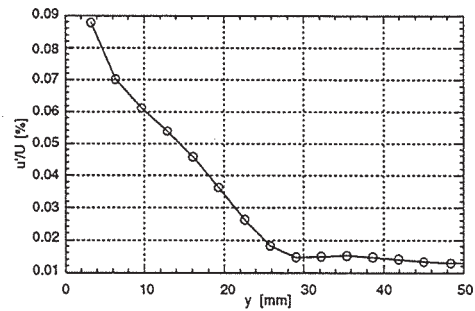


**Figure 6** Profile of turbulence intensity and fractional error in the estimation of the turbulence intensity

From sampling theory it can be derived that the fractional error in estimating the mean velocity value can be calculated from (Bendat 1986)

$$\epsilon_m = \frac{t}{\sqrt{N}} \frac{\sigma}{V} \quad \text{Equation 1}$$

where  $t$  is the value of Student's distribution,  $N$  the number of samples and  $\sigma/V$  the local turbulence intensity.

The fractional error for the standard deviation  $\sigma$  is given by

$$\varepsilon_\sigma = \frac{t}{\sqrt{2N}} \quad \text{Equation 2}$$

The number of samples required to obtain a given level of standard deviation is thus independent of the local turbulence level. Furthermore for turbulence levels smaller than 30 % it can be shown (Grant 1990) that the error in the estimation of the turbulence intensity is well approximated by the error in the standard deviation.

#### 4. Investigation of Three-Dimensional Flow using PIV

For the investigation of three-dimensional flow fields it needs to be taken into account that the PIV method in its traditional concept only determines the in-plane displacement of particles in a plane of light projected into the flow. For flows with a significant out-of-plane component the paraxial assumption for the imaging system encounters a systematic error with increasing distance from the principal optical axis (Lourenco 1986).

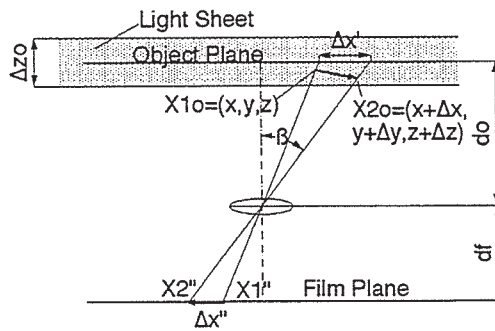


**Figure 7** Error in the measurements of in-plane displacements [Prasad A.K]

Figure 7 shows the situation as it appears in three-dimensional flows. Particles having a distinct out-of-plane motion  $\Delta z$  that are not located directly on the camera axis will yield recorded displacements  $\Delta x''$  ( $\Delta y''$ ) that do not match the true in-plane-displacements  $\Delta x$  ( $\Delta y$ ). They rather correspond to an apparent in-plane displacement  $\Delta x'$  ( $\Delta y'$ ) on the nominal object plane.

The relative error  $\varepsilon$  between the true and the apparent- in-plane displacement, can be given as (Prasad 1992).

$$\varepsilon = (\varepsilon_x, \varepsilon_y) = \left( \frac{\Delta x'}{\Delta x} - 1, \frac{\Delta y'}{\Delta y} - 1 \right) = \left( \frac{\Delta z}{\Delta x} \tan(\beta_x), \frac{\Delta z}{\Delta y} \tan(\beta_y) \right) \quad \text{Equation 3}$$

Whereas in terms of measured velocities the absolute error  $\delta$  can be expressed as.

$$\delta = (\delta_U, \delta_V) = (U' - U, V' - V) = (W * \tan(\beta_x), W * \tan(\beta_y)) \quad \text{Equation 4}$$

Equation 4 thus allows for a correction of three-dimensional flow effects in PIV measurements if the out-of-plane velocity is known. In the literature several stereoscopic PIV systems have been described (Hinsch 1995). All those systems are more or less capable of measuring the two instantaneous in-plane particle displacements and the out-of-plane velocity component. However a sophisticated calibration procedure is also needed to align the cameras to the field of view. This procedure generally becomes more complicated when stereoscopic PIV is applied to internal flow geometries. It is for this reason that for the study presented here a different approach was employed.

As mentioned in chapter 2 the test facility was designed in such a way that it allows a rotation of the test section around the flow streamwise axis without changing the flow conditions. The PIV measurements can therefore be carried out in perpendicular planes (see figure 8). Under the assumption of steady flow conditions the measurement planes can then be a combined yielding the three-dimensional mean velocity field. Figure 8 shows the location of the measurements planes for a typical series of measurements with 9 planes in each orientation.

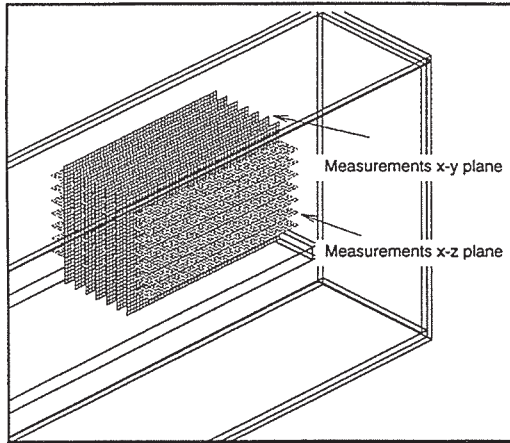


**Figure 8** Combination of perpendicular measurement planes

## 5. Results

In the following, some measurements carried out with the PIV system will be presented and the influence of the perspective error on the results will be discussed.

### 5.1 Two-Dimensional Developing Flow

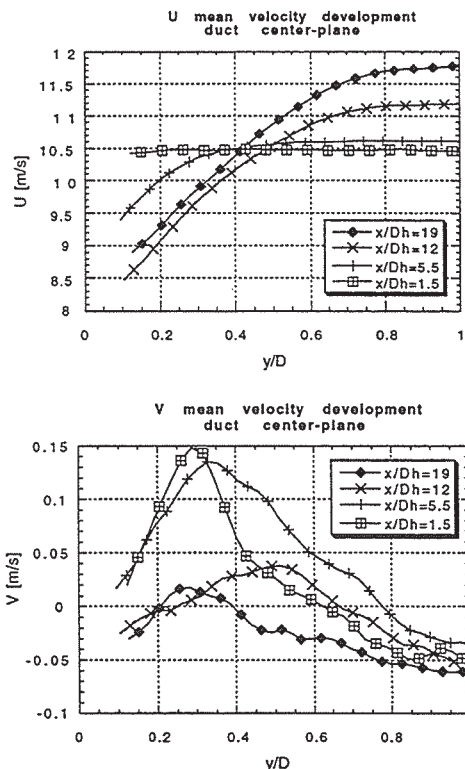


**Figure 9**  $U$  and  $V$  mean velocity development in a square duct ( $y/D=1$  equals half duct height)

The flow development in the center-plane was studied at four different axial

positions in a square duct with a length of 22 hydraulic diameters ( $Dh$ ).

During the development of the flow, the turbulent boundary layer grows to fill the entire cross section. The associated fluid motion from the wall towards the duct center can be seen in Figure 9.

As the flow develops, the peak in the transverse velocity component distribution moves towards the duct center indicating the location of the buffer zone between the core region and the boundary layer.

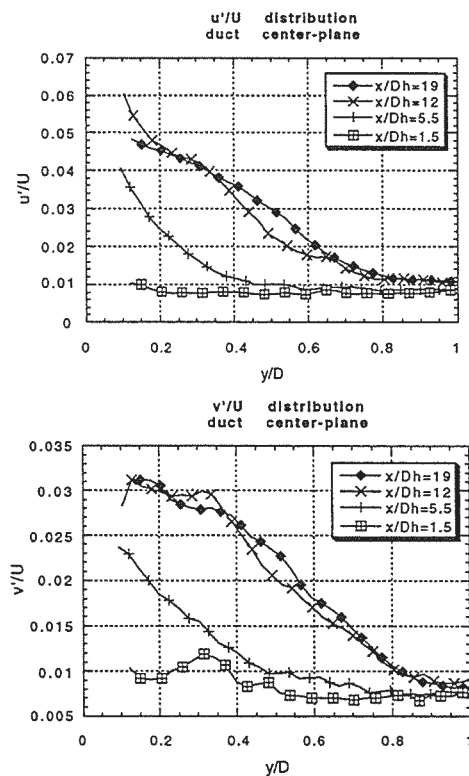


**Figure 10**  $u'/U$  and  $v'/U$  development in a square duct ( $y/D=1$  equals half duct height)

Figure 10 shows the development of the  $u'$ ,  $v'$  fluctuating velocities in the duct. At  $x/Dh=1.5$  low fluctuations of the order of 1% of the local mean velocity are observed. The fluctuating  $u'$  velocity increases up to a value of about 6% for the closest measuring point. The  $v'$  fluctuation follows the same trend, but remains at lower values close to the wall. Both the  $u'$  and the  $v'$  fluctuations approach the same value at the duct center-line.

## 5.2 Three-Dimensional Flow Upstream of a Sharp 180° Turn

The three-dimensional flow upstream of the turn in the cooling passage (see Figure 1) was investigated. Measurements in 9 parallel planes 10 mm apart were carried out. In each plane 35 PIV recordings were taken. The test section then was turned and the measurements were repeated. This procedure yields an ensemble of 18 planes that allow to reduce the three-dimensional steady flow field. The measurements were taken in a range from  $-0.65$  hydraulic diameter to  $0.15$  hydraulic diameter from the edge the turn. Figure 11 shows an example of the development of the  $U$  and  $W$  mean velocity in the vicinity of the turn.

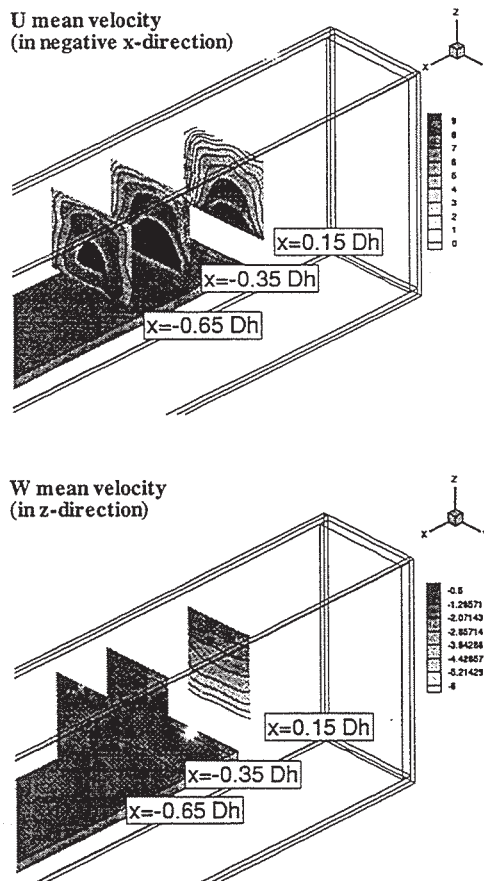


**Figure 11** Three-dimensional velocity field upstream of a  $180^\circ$  turn ( $D_h$ :hydraulic diameter)

The effect of the bend on the mean flow can already be observed at the first position shown ( $x/D_h = -0.65$ ). This is expressed in slight deformation of the  $U$

mean velocity distribution and a negative  $W$  mean velocity (see also Figure 12). As the flow approaches the turn region an acceleration of the streamwise mean velocity in the inner-radius half and deceleration of the mean velocity in the outer-radius half due to the pressure field in the turn can be observed. The velocity profiles in the  $xz$ -centerplane of the duct are shown in Figure 12.

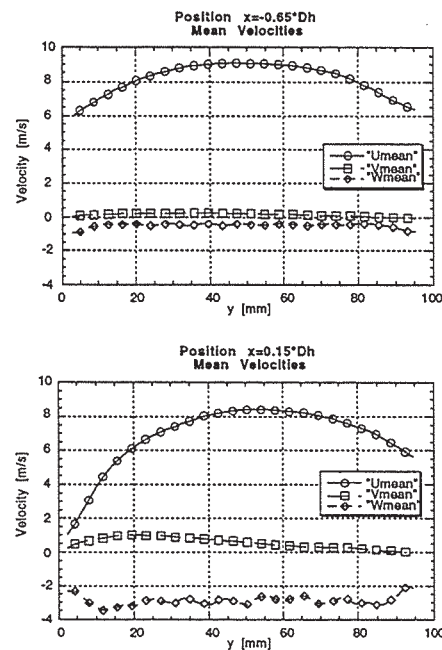


**Figure 12** Mean velocity profiles at two different positions relative to the turn leading edge

PIV measurements in three-dimensional flow are influenced by a systematic error as has been discussed in chapter 4. To quantify this error, the difference in the predicted  $U$  mean velocity from the measurement series (duct orientation  $xy$  and  $xz$ ) has been calculated (Figure 13). In regions of two-dimensional flow ( $x/D_h = -0.65$ ) an almost identical value of the streamwise mean velocity is predicted for both series of measurements. The differences in the velocities expressed by the curve  $\Delta U_{xy-xz}$  are likely due to the interpolation of the data matrices. Figure 13 supports the idea that consistent measurements can be obtained for different measuring days and orientations of the test section.

A significant difference in the streamwise velocity is found for measurements at  $x/D_h = 0.15$ .



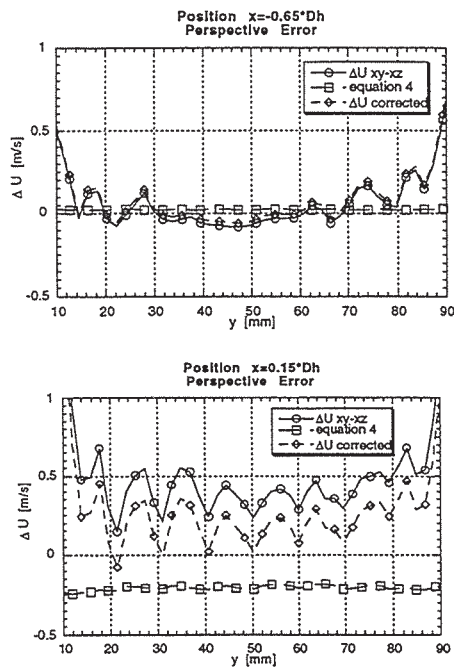


**Figure 13** Measurement error due to three-dimensional flow effects

At this position the out-of-plane velocity component reaches already values of 30% of the streamwise velocity and thus causes false measurements of the in-plane velocity components  $U$  and  $V$ .

A maximum error of 4% in the predicted streamwise velocity is observed. Equation 4 can be applied to the measurements yielding an improvement of the agreement between the two data sets. However, from Figure 13, it can also be seen that the correction due to equation 4 is not sufficient since a velocity difference on the order of 2% is still found. Reason for this is probably that the equation only takes into account the perspective error during the recording process and more specifically for the measurements of the instantaneous velocity field. For the study presented here the correction according to equation 4 was applied to the mean velocity data resulting in an underprediction of the perspective error. This shows the necessity of a velocity correction during the recording of the PIV images that can only be achieved by a stereoscopic PIV system.

## Conclusions

Instantaneous flow field measurements by means of the PIV method can be

used for statistical investigations. As a result mean flow fields and turbulence quantities can be obtained. The present paper describes the setup of a test rig and a PIV system for the study of the flow characteristics of three-dimensional flow in a model of an internal gas turbine cooling passage.

It was shown that even a relatively small number of PIV recordings allow the prediction of mean velocity components with relatively small uncertainty. For the reduction of turbulence quantities however a far larger number of recordings are required. The combination of measurements carried out in perpendicular planes furthermore allows the description of the three-dimensional features of the flow.

## References

- R.J. Adrian*  
Particle-Imaging Techniques for experimental fluid mechanics  
Annual Review of Fluid Mechanics, Vol 23 pp. 261-304 (1991)
- Hinsch K. D.*  
Three-dimensional particle velocimetry  
Meas. Sci. Technol. Vol. 6, pp. 742-753 (1995)
- Julius S. Bendat, Allan G. Piersol*  
Random Data  
Analysis and Measurement Procedures  
John Wiley & Sons
- Selected Papers on Particle Image Velocimetry*  
SPIE Milestone Series Volume MS 99
- Ian Grant, E.H. Owens*  
Confidence Interval estimates in PIV measurements of turbulent flows  
Appl. Optics. Vol. 29, pp. 1400-1402
- W. Lauterborn, A. Vogel*  
Modern optical techniques in fluid mechanics  
Annual Review of Fluid Mechanics, Vol. 16 pp. 223-244 (1984)
- Lourenco I. Whiffen M.C.*  
Laser speckle methods in fluid dynamics applications  
Laser Anemometry in Fluid Mechanics pp. 51-68 (1986)
- Prasad A.K. Adrian R.J*  
Stereoscopic particle image velocimetry applied to liquid flows  
Experiments in Fluids Vol. 15 pp. 49-60 (1993)